chemosensors

Supplementary

Proving Surface Plasmons in Graphene Nanoribbons Organized as 2D Periodic Arrays and Potential Applications in Biosensors

Talia Tene [1], Marco Guevara [2], Jiří Svozilík [3,4], Diana Coello-Fiallos [5], Jorge Briceño [6] and Cristian Vacacela Gomez [7,*]

[1] Department of Chemistry, Universidad Técnica Particular de Loja, Loja 110160, Ecuador
[2] Faculty of Mechanical Engineering, Escuela Superior Politécnica de Chimborazo (ESPOCH), Riobamba 060155, Ecuador
[3] Facultad de Ciencias, Escuela Superior Politécnica de Chimborazo (ESPOCH), Riobamba 060155, Ecuador
[4] Joint Laboratory of Optics of Palacký University and Institute of Physics of CAS, Faculty of Science, Palacký University, 17 listopadu 12, 771 46 Olomouc, Czech Republic
[5] Surface Nanoscience Group, Department of Physics, University of Calabria, Via P. Bucci, Cubo 33C, I-87036 Rende, Italy
[6] Dirección de Investigación y Vinculación, Universidad Estatal de Bolívar, Av. Ernesto Ché Guevara y Gabriel Secaira, CP. Guaranda 020150, Ecuador
[7] UNICARIBE Research Center, University of Calabria, I-87036 Rende, Italy
* Correspondence: cristianisaac.vacacelagomez@fis.unical.it

1. Supplementary Figures

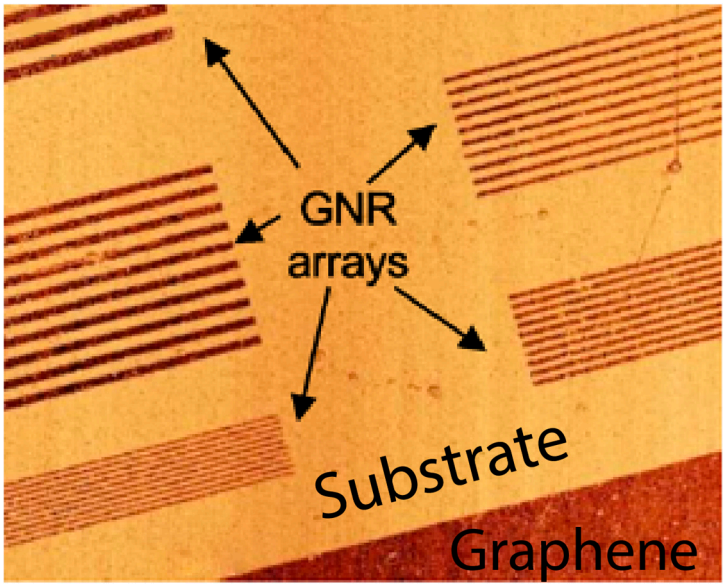

Figure S1. Experimentally realized graphene nanoribbons organized as 2D periodic arrays (Ref. [1]).

Citation: Tene, T.; Guevara, M.; Svozilík, J.; Coello-Fiallos, D.; Briceño, J.; Gomez, C.V. Proving Surface Plasmons in Graphene Nanoribbons Organized as 2D Periodic Arrays and Potential Applications in Biosensors. *Chemosensors* **2022**, *10*, 514. https://doi.org/10.3390/chemosensors10120514

Academic Editors: Iolanda Cruz Vieira, Edson Roberto Santana and João Paulo Winiarski

Received: 24 October 2022
Accepted: 30 November 2022
Published: 3 December 2022

Publisher's Note: MDPI stays neutral with regard to jurisdictional claims in published maps and institutional affiliations.

Copyright: © 2022 by the authors. Licensee MDPI, Basel, Switzerland. This article is an open access article distributed under the terms and conditions of the Creative Commons Attribution (CC BY) license (https://creativecommons.org/licenses/by/4.0/).

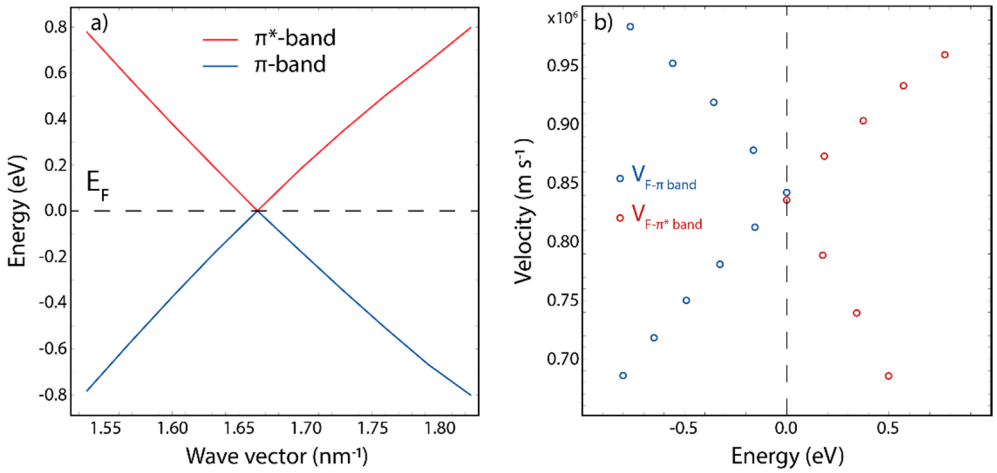

Figure S2. (**a**) Band structure of graphene in the vicinity of K point with the Fermi level set to zero energy. The blue line is the π band and the red line is the π^* band. (**b**) Fermi velocity as a function of the single-particle energy for the π band (blue circles) and the π^* band (darker red circles) in the k-point region.

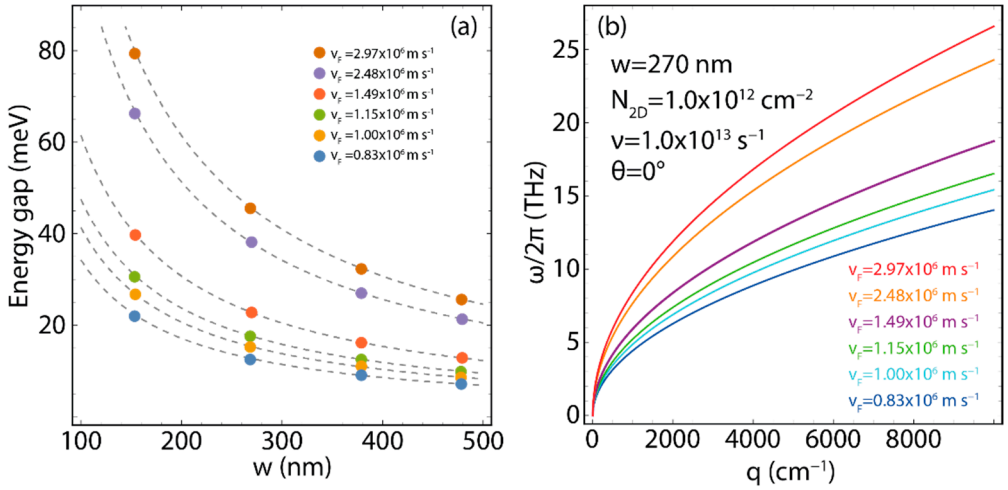

Figure S3. (**a**) Bandgap (Δ) as a function of the ribbon width (w). Markers represent the GNR systems under study and the dashed lines are the fitting curve using Equation 2. The numerical values of the bandgap are calculated using different charge carrier velocities as reported in Ref. [2]. (**b**) Plasmon frequency dispersion ($\omega/2\pi$) vs. wave vector (q) for 2D GNR arrays of $w = 270$ nm wide. The parameters of Equation 4 have been fixed as: $N_{2D} = 1.0 \times 10^{12}$ cm^{-2}, $\theta = 0$, $\nu = 1.0 \times 10^{13}$ s^{-1}, and different carrier velocities are considered.

2. Supplementary Tables

Table S1. Computed k-points and single-particle energies using LDA-DFT for the π and π^* bands close to the K point. Calculated Fermi velocity by Equation 2.

k-point (nm^{-1})	$E_{\pi-band}$(eV)	V_F (cm/s) 10^8	E_{π^*-band} (eV)	V_F (cm/s) 10^8
1.536	−0.765	0.985	0.796	0.960
1.568	−0.557	0.953	0.593	0.934
1.600	−0.357	0.920	0.397	0.904
1.632	−0.163	0.879	0.206	0.874
1.664	0.022	0.842	0.022	0.836
1.696	−0.155	0.813	0.198	0.789
1.728	−0.327	0.781	0.364	0.739
1.760	−0.491	0.750	0.520	0.685
1.792	−0.649	0.718	0.664	0.632
1.824	−0.800	0.686	0.797	0.577

Table S2. Bandgap and charge carrier effective mass of GNRs with ribbon width: $w = 155, 270, 380, 480$ nm. The free-electron mass is denoted as m_0. The charge carrier velocity is $v_F = 0.829 \times 10^6$ m/s.

Ribbon width (nm)	Bandgap (meV)	Effective mass (m^*)× m_0
155	22.12	2.83×10^{-3}
270	12.70	1.63×10^{-3}
380	9.02	1.16×10^{-3}
480	7.14	0.91×10^{-3}

Table S3. Bandgap and charge carrier effective mass of GNRs with ribbon width: $w = 155, 270, 380, 480$ nm. The free-electron mass is denoted as m_0. The charge carrier velocity is $v_F \approx 1.0 \times 10^6$ m/s.

Ribbon width (nm)	Bandgap (meV)	Effective mass (m^*)× m_0
155	26.68	2.35×10^{-3}
270	15.32	1.35×10^{-3}
380	10.88	0.96×10^{-3}
480	8.62	0.76×10^{-3}

Table S4. Peak position of plasmon response in 2D GNR arrays of 155, 270, 380, and 480 nm wide, selecting three different q values ($q = 100,\ 1000,\ 10{,}000$ cm^{-1}).

Ribbon width (nm)	q_{100} (THz)	q_{1000} (THz)	$q_{10,000}$ (THz)
155	1.03	3.35	10.63
270	1.38	4.43	14.03
380	1.64	5.26	16.65
480	1.85	5.91	18.71

Table S5. Percentage increase in plasmon frequency by increasing ribbon width for three different q values ($q = 100,\ 1000,\ 10{,}000$ cm^{-1}).

Ribbon width (nm)	q_{100} (%)	q_{1000} (%)	$q_{10,000}$ (%)
150 → 270	25.36	24.38	26.16
270 → 380	15.85	15.78	15.74
380 → 480	11.35	11.00	11.01

Table S6. Peak position of plasmon response in 2D GNR arrays of 155, 270, 380, and 480 nm wide, for selected q values at $\theta = 80$.

	w_{155} (THz)	w_{270} (THz)	w_{380} (THz)	w_{480} (THz)
q_{1000}		0.87	1.31	1.60
q_{2000}	1.05	1.75	2.23	2.59
q_{3000}	1.56	2.32	2.87	3.29
q_{4000}	1.94	2.78	3.39	3.86
q_{5000}	2.26	3.17	3.84	4.37
q_{6000}	2.54	3.52	4.25	4.81
q_{7000}	2.79	3.83	4.61	5.23
q_{8000}	3.02	4.12	4.96	5.61
q_{9000}	3.23	4.40	5.27	5.96
$q_{10,000}$	3.43	4.65	5.58	6.30

Table S7. Percentage increase in plasmon frequency by increasing ribbon width for three different q values ($q = 2000,\ 5000,\ 10{,}000$ cm^{-1}) at $\theta = 80$.

Ribbon width (nm)	q_{2000} (%)	q_{5000} (%)	$q_{10,000}$ (%)
150 → 270	39.85	28.71	26.24
270 → 380	21.52	17.45	16.67
380 → 480	13.90	12.13	11.43

Table S8. Peak position of plasmon response in 2D GNR arrays of 155, 270, 380, and 480 nm wide, for selected q values at $\nu = 4.0 \times 10^{13}$ s^{-1}.

	w_{155} (THz)	w_{270} (THz)	w_{380} (THz)	w_{480} (THz)
q_{100}				
q_{200}				0.86
q_{300}			1.53	2.24
q_{400}		1.35	2.40	3.05
q_{500}		2.06	3.02	3.69
q_{600}	0.69	2.58	3.54	4.23
q_{700}	1.36	3.01	3.99	4.71
q_{800}	1.80	3.39	4.40	5.15
q_{900}	2.15	3.72	4.77	5.55
q_{1000}	2.45	4.04	5.11	5.92

Table S9. Percentage increase in plasmon frequency by increasing ribbon width for three different q values ($q = 600,\ 800,\ 1000$ cm^{-1}) at $\nu = 4.0 \times 10^{13}$ s^{-1}.

Ribbon width (nm)	q_{600} (%)	q_{800} (%)	q_{1000} (%)
150 → 270	73.26	46.90	39.36
270 → 380	27.12	22.95	20.94
380 → 480	16.31	14.56	13.68

Table S10. Peak position of plasmon response in 2D GNR arrays of 155, 270, 380, and 480 nm wide, for selected q values at $N_{2D} = 4.0 \times 10^{12}$ cm^{-2}.

	w_{155} (THz)	w_{270} (THz)	w_{380} (THz)	w_{480} (THz)
q_{1000}	6.72	8.87	10.53	11.83
q_{2000}	9.51	12.55	14.89	16.73
q_{3000}	11.65	15.37	18.24	20.50
q_{4000}	13.45	17.75	21.05	23.67
q_{5000}	15.04	19.84	23.54	26.46
q_{6000}	16.47	21.74	25.79	28.99
q_{7000}	17.79	23.48	27.86	31.31
q_{8000}	19.02	25.10	29.78	33.47
q_{9000}	20.17	26.62	31.59	35.50
$q_{10,000}$	21.26	28.06	33.29	37.42

Table S11. Percentage increase in plasmon frequency by increasing ribbon width for three different q values ($q = 600,\ 800,\ 1000$ cm^{-1}) at $N_{2D} = 4.0 \times 10^{12}$ cm^{-2}.

Ribbon width (nm)	q_{1000} (%)	q_{5000} (%)	$q_{10,000}$ (%)
150 → 270	24.24	24.19	24.23
270 → 380	15.76	15.72	15.71
380 → 480	10.99	11.04	11.04

References

1. Fei, Z.; Goldflam, M.D.; Wu, J.-S.; Dai, S.; Wagner, M.; McLeod, A.S.; Liu, M.K.; Post, K.W.; Zhu, S.; Janssen, G.; et al. Edge and Surface Plasmons in Graphene Nanoribbons. *Nano Lett.* **2015**, *15*, 8271–8276.
2. Hwang, C.; Siegel, D.A.; Mo, S.-K.; Regan, W.; Ismach, A.; Zhang, Y.; Zettl, A.; Lanzara, A. Fermi Velocity Engineering in Graphene by Substrate Modification. *Sci. Rep.* **2012**, *2*, 590.